FGF signalling controls expression of vomeronasal receptors during embryogenesis

Oleg Lioubinski[1], Maria Teresa Alonso[1,2], Yolanda Alvarez[1], Victor Vendrell[3], Manuel Garrosa[4], Paula Murphy[3] and Thomas Schimmang[1,2]

[1]Center for Molecular Neurobiology, University of Hamburg, Falkenried 94, D-20251 Hamburg, Germany

[2]Instituto de Biología y Genética Molecular, Universidad de Valladolid y Consejo Superior de Investigaciones Cientificas, E-47003 Valladolid, Spain

[3]Zoology Department, Zoology Building, Trinity College Dublin, Dublin 2, Ireland

[4]Department of Cell Biology and Institute of Neuroscience of Castilla y Leon, Faculty of Medicine, University of Valladolid, 47005 Valladolid, Spain

Running title: Embryonic expression of vomeronasal receptors

Key words: Fibroblast growth factor, vomeronasal organ, V2R, dorsal root ganglia, inner ear

Corresponding author: Dr. Thomas Schimmang

IBGM, Faculty of Medicine

C/Ramon y Cajal 7

47005 Valladolid

Spain

Tel.: +34983423609

Fax: +34983423588

Email: schimman@ibgm.uva.es

Number of figures: 4

Number of references:47

Abstract

Fibroblast growth factors (FGFs) have been shown to control formation and differentiation of multiple organ systems in the developing vertebrate embryo. The analysis of differential gene expression during embryogenesis is therefore a potent tool to identify novel target genes regulated by FGF signalling. Here, we have applied microarray analysis to identify differentially regulated genes in FGF mutant mouse embryos. Surprisingly, transcripts corresponding to vomeronasal receptors (VRs), which so far have been only detected in the vomeronasal organ (VNO), were found to be downregulated in FGF mutant embryos. VR expression was detected in the developing olfactory pit and the anlage of the VNO. Interestingly, several FGFs can be detected in the developing olfactory pit during mouse embryogenesis (Bachler and Neubüser, 2001). FGF signalling may thus control expression of VRs in the olfactory pit and formation of the VNO. Moreover, VR expression was detected in unexpected locations within the developing embryo including retina, dorsal root ganglia and neural tube. The relevance of VR expression in these structures and for formation of the VNO is discussed.

Introduction

Fibroblast growth factors (FGFs) make up a family of polypeptide growth factors found throughout the animal kingdom. During embryonic development, they regulate cell proliferation and differentiation, body plan formation and organogenesis (Ornitz and Itoh, 2001; Reuss and von Bohlen und Halbach., 2003). Several FGF members, among them FGF3, FGF8, FGF10 and FGF19, have been implicated in different stages of inner ear development (Barald and Kelley, 2004; Ladher et al., 2005). The stage of the otic vesicle (otocyst) is of high importance for inner ear development, because at this time point the inner ear undergoes subdivision into defined compartments, ultimately leading to the generation of the highly complex differentiated organ (Brigande et al., 2000). This process of regionalization and specification is very likely to be regulated by different genetic pathways. Indeed, previous studies, based on a cDNA subtraction screening technique, have identified numerous candidate genes potentially involved in controlling patterning of the inner ear at the otocyst stage (Powles et al., 2004). Recently, it was shown that FGF3 and FGF10 synergistically control formation of the otic vesicle in mice (Alvarez et al., 2003; Wright and Mansour, 2003). Since next to the inner ear, FGF3 and FGF10 have been shown to control the formation of other embryonic structures, including lung, limbs and tail (Mansour et al., 1993; Min et al., 1998; Sekine et al., 1999) during mouse development, mouse mutants for these FGF genes may serve as an ideal tool to identify novel downstream effectors of FGF signaling.

The vomeronasal organ (VNO) originates from the medial wall of the olfactory (nasal) pit where the VNO anlage is induced as a bud which will form the vomeronasal groove (Garrosa et al., 1998). In adult mammals, the mature VNO located in the nasal septum contains sensory neurons, which project their axons to the accessory olfactory bulb (AOB). In turn, neurons of the AOB project to discrete loci within the vomeronasal amygdala (Halpern, 1987). After direct contact with pheromone sources, these non-volatile chemicals enter the VNO and elicit

complex behavioral responses. It is believed that the pheromone molecules are bound by vomeronasal receptors (VRs) from the multigene family of G-protein-coupled receptors, which trigger a phospholipase C (PLC)-dependent signal cascade (Holy et al., 2000). The mature VNO is organized into two distinct layers. Vomeronasal receptor neurons with cell bodies in the apical part of the sensory epithelium express the G-protein α-subunit $G\alpha_{i2}$ and project to the anterior part of the AOB, whereas basally located neurons of the VNO express the G-protein α-subunit $G_{o\alpha}$ and project to the posterior region of the AOB (Berghard and Buck, 1996, Jia et al., 1997, Shinohara et al., 1992). In addition, apical neurons express receptors of the V1R family, whereas basal sensory neurons express those of the V2R family. Each of these VR multigene families comprises more than a hundred genes (Dulac and Torello, 2003), thereby adding significant complexity to the analysis of individual VR genes. Recently, it was shown that small peptides which serve as ligands for major histocompatibility complex (MHC) class I molecules can stimulate V2R receptors (Leinders-Zufall et al., 2004).

In the present report we have used microarrays to screen for novel targets of FGF signaling by hybridising them with cDNAs derived from FGF3, FGF10 and homozygous compound mutants for these genes. As expected we found genes normally expressed in the otic vesicle to be downregulated in FGF mutants. Unexpectedly however, we also found transcripts derived from the V2R gene family to be downregulated in these mutants. Expression of V2R transcripts was detected in the olfactory pit, retina, dorsal root ganglia (DRG) and neural tube of mouse embryos. FGFs thus appear to control early expression of V2Rs in the developing embryo. These results suggest potential roles of FGF signaling during formation of the VNO and other embryonic structures expressing V2R transcripts.

Results

A microarray-based screen for FGF-regulated genes

FGF3 and FGF10 have been shown to control formation of the otic vesicle in mice (Alvarez et al., 2003; Wright and Mansour, 2003). Double mutant homozygous *Fgf3*$^{-/-}$/*Fgf10*$^{-/-}$embryos lack otic vesicles or only form microvesicles at the otic vesicle stage from embryonic day 9 (E9) to E10. To reveal the genes regulated by FGF signaling during embryogenesis we employed gene chips covering the expression of 36.000 known mouse genes and expressed sequence tags (U74ABC V.2 set from Affymetrix; see methods). Due to the very limited amount of otic tissue in *Fgf3*$^{-/-}$/*Fgf10*$^{-/-}$ mutants we opted to isolate RNA from embryonic tissue at E10 corresponding to the area of the otic vesicle and neighbouring tissue, including periotic mesenchyme and the neural tube (see methods). Both of the latter tissues have been shown to be essential for formation of the inner ear and influence the expression of otic genes (Baker and Bronner-Fraser, 2001). In our analysis, we compared three groups of embryos against their wild-type littermates: *Fgf3*$^{-/-}$, *Fgf10*$^{-/-}$, and double *Fgf3*$^{-/-}$/*Fgf10*$^{-/-}$ mutants (see methods). As a result, a list of genes, which showed altered expression levels in the absence of FGFs, was generated. We discovered genes already reported to have expression in the otic vesicle, as well as genes not previously implicated during inner ear development (see below). We further focused our analysis on a set of selected genes downregulated in the FGF-deficient embryos, as presented in Figure 1. These genes corresponded to *retinaldehyde-dehydrogenase 1* (*Aldh1 (Raldh1)*; Romand et al., 2004), *chromobox homolog 3* (*Cbx3*; Jones et al., 2001), *myeloblastosis oncogene-like 1* (*Mybl1*; Trauth et al., 1994), *otoconin 90* (*Oc90 (Oc95)*; Wang et al., 1998; Verpy et al., 1999) and vomeronasal receptors (V2Rs; Herrada and Dulac, 1997; Matsunami and Buck; 1997; Ryba and Tirindelli; 1997). A complete list of the microarray results obtained from the hybridizations of the U74A V.2 chips can be found in the supplementary information.

To analyse more globally in the developing embryo the differential expression of the selected genes with an independent technique, we next employed semi-quantitative reverse-transcriptase polymerase chain reaction (RT-PCR). We extracted total RNA from wild-type, *Fgf3*$^{-/-}$, *Fgf10*$^{-/-}$ and *Fgf3*$^{-/-}$/*Fgf10*$^{-/-}$ embryos at E10, which then served as a template in a one-step RT-PCR with gene-specific primers (see methods). RNA amounts in samples were normalized by using two independent housekeeping genes, *beta-actin* and *glyceraldehyde 3-phosphate dehydrogenase* (*gapdh*). Among the genes we analyzed by RT-PCR, we found *Aldh1* and *V2Rs* to be downregulated in single and compound FGF mutants (Fig.2 A, C), while *Oc90* was only downregulated in *Fgf3*$^{-/-}$/*Fgf10*$^{-/-}$ double mutants (Fig. 2 B), consistent with the results from the gene chips (Fig.1). In contrast, *Cbx3* and *Mybl1* failed to show a significant change in mRNA levels between wild-type and FGF mutant embryos (data now shown).

Downregulation of vomeronasal receptors in FGF mutant embryos

Surprisingly, some of the most strongly FGF-regulated genes turned out to be transcripts corresponding to vomeronasal receptor genes. So far, expression of vomeronasal receptors has been reported only in the vomeronasal organ (VNO), which is part of the vomeronasal system responsible for the molecular detection of pheromone signals (Dulac and Torello, 2003). Two large families of genes encoding pheromone receptors (V1Rs and V2Rs) have been described (Dulac and Axel; 1995; Herrada and Dulac, 1997; Matsunami and Buck; 1997; Ryba and Tirindelli; 1997). Initially, we detected several members of the V2R family (V2R1, V2R2, V2R8, V2R9, V2R12) downregulated on the gene chips (See Figure 1 and data not shown). In contrast, all genes of the V1R family which were represented on the gene chips displayed no significant changes (data not shown). At a closer look, we discovered that all oligos used on the Murine Genome U74A Chip representing the V2R family, were selected

from a 450-bp stretch that bore 100% to 98,5% identity between the V2R genes. Therefore, expression of even a single V2R gene from this group would produce a positive signal for all of them. It was thus unclear, whether indeed only a single or a subset of *V2R* genes were differentially expressed. Therefore, we refer to the differentially regulated vomeronasal receptors as "V2Rs", indicating the possibility of multiple gene products. To clarify the identity of V2R transcripts, we subcloned the V2R RT-PCR products amplified from total RNA from E10 embryos. Importantly, in the RT-PCRs we observed a single discrete band corresponding to the expected size of 417 nucleotides of the RT-PCR fragment amplified from V2Rs using primers whose sequences were conserved between the V2Rs found to be differentially expressed (Fig. 2C). Bacteria were transformed with a mix of plasmids bearing the PCR products as an insert, and individual clones were subjected to sequencing. After processing twenty clones we discovered that either of two V2Rs were present, highly homologous V2R8 and V2R9. Therefore it appears likely that at least some of the V2R transcripts found to be differentially expressed in FGF mutants are derived from the V2R8 and V2R9 genes, which both belong to the family B of V2R receptors (Yang et al., 2005).

Embryonic expression pattern of V2R-related transcripts

To examine the spatial expression pattern of V2R genes in the developing embryo, we generated an in situ probe from the 450 bp nucleotide sequence corresponding to V2Rs on the gene chip and analyzed the expression pattern on E8.5-E12 mouse embryos using RNA in situ hybridization and optical projection tomography (OPT; see methods). V2R expression was observed between E10-E12 in various parts of the developing embryo, including dorsal root ganglia (DRGs), neural tube, retina and olfactory pit (Fig. 3B-G). In DRGs, intense V2R expression was observed at E10 but was found to be downregulated at E12 (Fig. 3B,C and data not shown). In the olfactory pit, V2R expression was initially observed in the lateral wall

at E10 (Fig. 3E). At E11.75 V2Rs maintained this expression domain, but additionally transcripts were detected in the vomeronasal anlage which forms and starts to invaginate in the medial part of the olfactory pit (Fig. 3F,G).

To reconfirm the presence and differential expression of V2Rs in these novel and unexpected sites in the developing embryo we isolated RNA from DRGs, which can be easily isolated from E12 onwards (see methods). We thus prepared DRGs from E13 wild-type and *Fgf10*$^{-/-}$ mutants and performed RT-PCR using V2R primers. We could confirm presence of the V2R transcript and its downregulation in DRGs from *Fgf10*$^{-/-}$ mutants compared with the wild-type (Fig. 2D). We were further interested to define if DRGs indeed expressed V2R8 transcripts as suggested by the sequence analysis of the V2R transcripts amplified by PCR (see above). Using gene-specific primers, we could confirm presence of V2R8 transcripts in DRGs and their downregulation in *Fgf10*$^{-/-}$ mutants (Fig. 2E).

Development of the vomeronasal organ in FGF mutants

To determine if V2R8(V2R)-downregulation by FGF signaling leads to any defects in the VNO, we examined the phenotype of the VNO in FGF mutants. Since FGF10 mutants die at birth we chose *Fgf3*$^{-/-}$ and compound *Fgf3*$^{-/-}$/*Fgf10*$^{+/-}$ mutants for histological analysis of the VNOs. No abnormalities in organ morphology or neuronal appearance were detected at E18 and in adult animals (Figure 4A,B and data not shown). The number of basally located neurons expressing V2R genes was also normal, as confirmed by immunohistochemical staining with an antibody against V2R2, which was previously shown to label all basal VNO neurons (Fig. 4C,D; Martini et al., 2001). At the molecular level, we did not observe any decrease in V2R8 gene levels by RT-PCR in adult VNO RNA from *Fgf3*-deficient mice as well as compound *Fgf3*$^{-/-}$/*Fgf10*$^{+/-}$ mutants (data not shown). These results were also confirmed with the V2R primers, directed against various family members of the V2R gene

family. Likewise, male-male aggression (resident-intruder test) and mating behavior controlled by the VNO showed no apparent changes in *Fgf3*-deficient mice (data not shown). Slightly less efficient mating in compound *Fgf3*$^{-/-}$/*Fgf10*$^{+/-}$ mutants was attributed to their idiopathic weight reduction and smaller size. Therefore, downregulation of V2R transcripts in FGF mutant embryos appears not to affect morphology or functionality of the VNO.

Discussion

Downregulation of otic genes in FGF mutants

Next to the unexpected finding of V2R downregulation in FGF mutant embryos, the loss of two genes known to be expressed in the inner ear could also be confirmed. Otoconin-90/95 is the major component of otoconia of the inner ear (Wang et al., 1998; Verpy et al., 1999). Importantly, otoconin-90 is exclusively expressed in the otic vesicle at E10 (Verpy et al., 1999), which underscores the achievement of one of our aims to identify genes specific to the otic vesicle altered in FGF mutants during embryogenesis. In the case of otoconin-90/95 the downregulation is only observed in *Fgf3*$^{-/-}$/*Fgf10*$^{-/-}$ double mutants which is most likely explained by the severe loss of otic tissue in these mutants at E10 (Alvarez et al., 2003; Wright and Mansour, 2003).

Expression of *Raldh1* has been described in the dorsal-medial part of the otic vesicle which gives rise to the endolymphatic duct and parts of the vestibular system (Haselbeck et al., 1999; Romand et al., 2004). Loss of the endolymphatic duct and defects in the vestibular system have been described in a FGF3 mouse mutant (Mansour et al., 1993) and/or FGF10 mouse mutants (Pauley et al., 2003; Ohuchi et al., 2005), indicating that *Raldh1* may participate in the morphogenesis of these inner ear structures. However, no inner ear phenotypes have been reported so far in *Raldh1* knockout mice (Fan et al., 2003).

Does loss of FGF signaling affect formation of the VNO?

In the present report we have detected V2R transcripts in several structures of the developing mouse embryo and found these transcripts to be downregulated in FGF mutant embryos. Is there a link between FGF signaling, expression of V2R transcripts and formation of the VNO? In mice, the VNO develops from a thickening within the olfactory pit at around E11 (Cuschieri and Bannister, 1975). Interestingly, we observed expression of V2R transcripts within the olfactory pit between E10 and E12. At this timepoint the expression of several FGFs, including FGF3 and FGF10 have also been described in the olfactory pit (Bachler and Neubüser, 2001). Notably at E10, FGF3 expression is present in the medial part of the olfactory pit where the VNO anlage will form and where V2R expression is detected at E11.75. On the other hand, FGF10 expression overlaps with V2R expression in the lateral part of the olfactory pit at E10. Therefore, a combinatorial expression pattern of FGFs may be important to control V2R expression in the olfactory pit during development. We have obtained no evidence for molecular or morphological changes in the mature VNO of FGF mouse mutants. A possible explanation for this may be the presence of redundant pathways of FGF signaling controlling V2R expression and formation of the VNO. Consistent with this hypothesis mouse mutants for FGFR1, a high-affinity receptor for FGF3 and FGF10, show defects during development of the VNO (A. Neubüser, personal communication). It will therefore be interesting to further elucidate which FGF ligands participate in VNO formation and how they control V2R expression. One of the key factors for VNO formation may be FGF8 which is highly expressed in the olfactory pit (Bachler and Neubuser, 2001) and has been shown to control facial morphogenesis most likely via the expression of several downstream targets, possibly also including members of the retinaldehyde dehydrogenase enzyme family (Trumpp et al., 1999; Finberg and Neubüser, 2002; Song et al., 2004; see also above). Preliminary studies of mouse mutants homozygous for FGF3 and heterozygous for FGF8 (*Fgf3*$^{-/-}$/*Fgf8*$^{+/-}$) show a severe loss of aggressive behaviour between adult males in the

resident-intruder test, consistent with a defect in the VNO (M. T. Alonso and T. Schimmang, unpublished results). Therefore, further studies of these mutants may reveal important insights in the role of FGF signaling for formation and functional differentiation of the VNO.

Is there are molecular basis for V2R signaling during embryonic development?

In the present article we have described V2R expression in a number of unexpected sites in the developing embryo, including the retina, neural tube and DRGs. V2R receptors functionally associate with MHC I molecules and β2-microglobulin and are coupled to $G_{o\alpha}$ proteins (Berghard and Buck, 1996; Loconto et al., 2003; Dulac and Torello, 2003). It is noteworthy that both MHC I molecules and β2-microglobulin are expressed in the developing embryo (Jaffe et al., 1990; Jaffe et al., 1991), including DRGs (Neumann et al., 1997). Our preliminary analysis of $G_{o\alpha}$ expression in the developing mouse has also revealed presence of $G_{o\alpha}$ transcripts in the DRGs and neural tube (O. Lioubinski, unpublished observation). Therefore, certain signaling components of the cascade triggered by V2R receptors may indeed be present during embryonic development. V2Rs may thus perform as yet unknown cellular functions in neural structures outside of the VNO. Interestingly, MHC I molecules which can associate with V2Rs have been shown to control neuronal differentiation and plasticity during development (Boulanger and Shatz, 2004). Therefore, V2Rs may also transiently participate in control of neural functions during embryonic development. Further studies will be required to clarify the potential role of V2Rs during embryogenesis outside the VNO.

Experimental Procedures

CHIP hybridizations

RNA was prepared from otic vesicles and neighbouring tissues, including the neural tube and periotic mesenchyme of embryos at E10 (see Fig. 3A). Two independent RNA samples were obtained from a total of ten embryos of each of the following genotypes: wild-type, *Fgf3*$^{-/-}$, *Fgf10*$^{-/-}$ and *Fgf3*$^{-/-}$/*Fgf10*$^{-/-}$ mutants. RNA preparation, hybridization to oligonucleotide arrays (U74ABC, version 2) and scanning of the arrays was performed as described in the Affymetrix GeneChip Expression Analysis Manual (http://www.affymetrix.com). Scanned files were analyzed with GeneChip (Affymetrix) and the expression data were saved as an Excel file containing expression values (Average Difference). Results from the hybridisations of U74A V.2 microarrays can be found in the supplementary information and at ArrayExpress (http://www.ebi.ac.uk/arrayexpress/) under accession number E-MEXP-430.

Semi-quantitative RT-PCR

For semi-quantitative RT-PCR, RNA was extracted from whole embryos or dorsal root ganglia with TRIZOL reagent (Invitrogen), digested in solution with DNaseI (Roche), and purified with RNAeasyKit, including a second DNaseI digestion step (on-column). Absence of genomic DNA contamination was confirmed by RT-PCR with primers against mouse *pdx-1* gene. For this, the forward primer was chosen from the exonic, and the reverse in the intronic region. A 150-bp band would be produced only in case of genomic DNA traces in the sample. Following these steps, RNA was used as template for RT-PCR (Qiagen OneStep RT-PCR Kit). RNA was diluted such that the intensity of the *beta-actin* PCR product bands of all RNA samples was equal at their earliest visible cycle. RNA calibration was then confirmed by RT-PCR with primers against another housekeeping gene, *glyceraldehyde 3-phosphate dehydrogenase* (*gapdh*). After calibration, RT-PCRs with gene-specific primers were performed simultaneously with RT-PCR for *beta-actin*. Aliquots of PCR mixes were removed

at multiple points in the cycles, applied on an agarose gel, and DNA bands were visualized by ethidium bromide. Band intensities were compared to each other at the lowest number of cycles at which products started to be visible. The following primers were used (all sequences from *mus musculus*): *beta-actin* (Genebank accession Nr. NM_007393): forward 5'-TGTGATGGTGGGAATGGGTCAG-3', reverse 5'-TTTGATGTCACGCACGATTTCC-3', *Aldh1* (NM_013467): fw 5'-CTGGGCTGACAAGATTCATGGTCA-3', rev 5'-GGTGAAGAGCCGTGAGAGGAGTTT-3', *Cbx3* (NM_007624): fw 5'-ATGCTGATAATACTTGGGAACCAG-3', rev 5'-GTAGAAGGCAATGACAATCTGAGG-3', *Mybl1* (NM_008651): fw 5'-ctcatggatgatagtatgtctaaca-3', rev 5'-GGATGTTAAAGGAATAGCTTCACTG, *Oc90* (NM_010953): fw 5'-CTGCTGTTTGGAGCAGATGAGACAA-3', rev. 5'-TCCGTCTGGTGACTTGAGGCTTTGA-3', *Pdx1* (NM_039324): fw 5'-CCAGTGGGCAGGTAAGCCT-3', rev 5'-TCCTAGCCTCGATTATCCTTGC-3', V2R (multiple sequences): fw 5'-GTTGCTAATGTGTATCTTTGTCCCA-3', rev 5'-TCATGTCCATTGTGTATGCAGTACC-3', V2R8 (NM_009494): fw 5'-CTCCTCCGTGTGTAGTGTGG-5', rev 5'-GCTGAGAATGCGGTTATTGG-3', (V2R9 (NM_009495): fw 5'-CAGACATGAAGAAGCTCTGTGC-3', rev 5'-GGATTCCTGTTGATCTCATCG-3'.)

RNA in situ hybridization analysis

RNA whole-mount in situ hybridization was essentially performed as described by Conlon and Rossant (Conlon and Rossant, 1992) using digoxigenin-labelled riboprobes, which were detected by alkaline phosphatase-coupled antibodies. For histological examination, embryos were postfixed in 4% PFA, embedded in gelatin and sectioned at 30 µm on a vibratome. For whole-mount RNA in situ hybridization a V2R2 antisense-riboprobe corresponding to nucleotides 2416 to 2832 of the V2R2 cDNA (accession number AF011412) was used.

Optical Projection Tomography (OPT)

After RNA in situ hybridsation embryos were fixed overnight (o/n) in 4% PFA at 4°C, rinsed briefly in destilled water and embedded in pre-warmed low melting agarose (1% in water). Once the agarose had solidified at room temperature (RT), blocks were cut and dehyrated in methanol at RT o/n. After dehydration of the agarose blocks, specimens were cleared in BABB (Benzyl alcohol/ Benzyl benzoate, 1:2) for one or two days. The specimens were scanned with an OPT Scanner (provided by the MRC Human Genetics Unit, Edinburgh). Scans were performed in a bright field channel using 700 or 750 nm filters. The 3D reconstructions were performed as described by Sharpe et al. (2002). Images of virtual sections shown here were captured directly from the 3D reconstructions.

Isolation of dorsal root ganglia

Dorsal root ganglia from embryos were isolated as described by Kleitmann et al., (1998).

Histology and Immunohistochemistry

For light microscopy, adult mice were anesthetized with ketamine sulphate and transcardially perfused with 4% paraformaldehyde in phosphate buffer. The noses were removed and left in 10% EDTA solution for decalcification. Afterwards, pieces were processed for paraffin embedding. Sectioning of paraffin blocks was carried out with a Minot microtome at 7 µm and sections were stained with hematoxylin and eosin. Immunohistochemistry on adult VNOs using V2R2 antibodies was performed as described by Martini et al. (2001).

Acknowledgements

This work is dedicated to María Gómez Gómez. We thank Annette Neubüser, Sybille Köhnke and Michaela Miehe for communicating unpublished results, help in genotyping mice and analyzing results of the microarrays, respectively. V2R2-antibodies and *Fgf10*$^{-/-}$ mutants were

a generous gift from Roberto Tirindelli and Shigeaki Kato, respectively. This work has been generously supported by Deutsche Forschungsgemeinschaft (SFB444) and grant BFU2004-00860 of the Spanish MEC.

Literature

Alvarez, Y., Alonso, M.T., Vendrell, V., Zelarayan, L.C., Chamero, P., Theil, T., Bösl, M.R., Kato, S., Maconochie, M., Riethmacher, D., Schimmang, T. 2003. Requirements for FGF3 and FGF10 during inner ear formation. Development 130, 6329-6338.

Bachler, M., Neubuser, A. 2001. Expression of members of the Fgf family and their receptors during midfacial development. Mech. Dev. 100, 313-316.

Baker, C.V., Bronner-Fraser, M. 2001. Vertebrate cranial placodes I. Embryonic induction. Dev. Biol. 232, 1-61.

Barald, K.F., Kelley, M.W. 2004. From placode to polarization: new tunes in inner ear development. Development. 131, 4119-4130.

Berghard, A., Buck, L.B. 1996. Sensory transduction in vomeronasal neurons: Evidence for g alpha o, g alpha i2, and adenylyl cyclase II as major components of a pheromone signaling cascade. J. Neurosci. 16, 909-918.

Boulanger, L.M., Shatz, C.J. Immune signalling in neural development, synaptic plasticity and disease. Nat. Rev. Neurosci. 5, 521-531.

Brigande, J.V., Kiernan, A.E., Gao, X., Iten, L.E., Fekete, D.M. 2000. Molecular genetics of pattern formation in the inner ear: do compartment boundaries play a role? Proc. Natl. Acad. Sci. USA. 97, 11700-11706.

Conlon, R.A., Rossant, J. 1992. Exogenous retinoic acid rapidly induces anterior ectopic expression of murine Hox-2 genes in vivo. Development. 116, 357-368.

Cuschieri, A., Bannister, L.H. 1975. The development of the olfactory mucosa in the mouse: Light microscopy. J. Anat. 119, 277-286.

Dulac, C., Axel, R. 1995. A novel family of genes encoding putative pheromone receptors in mammals. Cell 83, 195-206

Dulac, C. and Torello, A.T. 2003. Molecular detection of pheromone signals in mammals: From genes to behaviour. Nat. Rev. Neurosci. 4, 551-562.

Fan, X., Molotkov, A., Manabe, S., Donmoyer, C.M., Deltour, L., Foglio, M.H., Cuenca, A.E., Blaner, W.S., Lipton, S.A., Duester, G. 2003. Targeted disruption of Aldh1a1 (Raldh1) provides evidence for a complex mechanism of retinoic acid synthesis in the developing retina. Mol. Cell. Biol. 23, 4637-4648

Firnberg, N., Neubuser, A. 2002. FGF signaling regulates expression of Tbx2, Erm, Pea3, and Pax3 in the early nasal region. Dev. Biol. 247, 237-250.

Garrosa, M., Gayoso, M.J., Esteban, F.J. 1998. Prenatal development of the mammalian vomeronasal organ. Microscopy Res. Tech. 41, 456-470.

Halpern, M. 1987. The organization and function of the vomeronasal system. Annu. Rev. Neurosci. 10, 325-362.

Haselbeck, R.J., Hoffmann, I., Duester, G. 1999. Distinct functions for Aldh1 and Raldh2 in the control of ligand production for embryonic retinoid signaling pathways. Dev. Genet. 25, 353-364.

Herrada, G., Dulac, C. 1997. A novel family of putative pheromone receptors in mammals with a topographically organized and sexually dimorphic distribution. Cell 90, 763-773.

Holy, T.E., Dulac, C., Meister, M. 2000. Responses of vomeronasal neurons to natural stimuli. Science 289, 1569-1572.

Jaffe, L., Jeannotte, L., Bikoff, E.K., Robertson, E.J. 1990. Analysis of beta 2-microglobulin gene expression in the developing mouse embryo and placenta. J. Immunol. 145, 3474-3482.

Jaffe, L., Robertson, E.J., Bikoff, E.K. 1991. Distinct patterns of expression of MHC class I and beta 2-microglobulin transcripts at early stages of mouse development. J. Immunol. 147, 2740-2749.

Jia, C., Goldman, G., Halpern, M. 1997. Development of vomeronasal receptor neuron subclasses and establishment of topographic projections to the accessory olfactory bulb. Brain Res. Dev. Brain Res. 102, 209-216.

Jones, DO., Mattei, M.G., Horsley, D., Cowell, I.G., Singh, P.B. 2001. The gene and pseudogenes of Cbx3/mHP1 gamma. DNA Seq. 12, 147-160.

Kleitmann, N., Wood, P.M., Bunge, R.P. 1998. Tissue culture methods for the study of myelination in culturing nerve cells in Banker, G and Goslin, K. (Eds.), Culturing Nerve Cells, MIT press, pp. 545-594.

Ladher, R.K., Wright, T.J., Moon, A.M., Mansour, S.L., Schoenwolf, G.C. 2005. FGF8 initiates inner ear induction in chick and mouse. Genes Dev. 19, 603-613.

Leinders-Zufall, T., Brennan, P., Widmayer, P., Prashanth Chandramani, S., Maul-Pavicic, A., Jager, M., Li, X.H., Breer, H., Zufall, F., Boehm, T. 2004. MHC class I peptides as chemosensory signals in the vomeronasal organ. Science 306, 1033-1037.

Loconto, J., Papes, F., Chang, E., Stowers, L., Jones, E.P., Takada, T., Kumanovics, A., Fischer Lindahl, K., Dulac, C. 2003. Functional expression of murine V2R pheromone receptors involves selective association with the M10 and M1 families of MHC class Ib molecules. Cell 112, 607-618.

Mansour, S.L., Goddard, J.M., Capecchi, M.R. 1992. Mice homozygous for a targeted disruption of the proto-oncogene int-2 have developmental defects in the tail and inner ear. Development. 117, 13-28.

Martini, S., Silvotti, L., Shirazi, A., Ryba, N.J. and Tirindelli, R. 2001. Co-expression of putative pheromone receptors in the sensory neurons of the vomeronasal organ. J. Neurosci. 21, 843-848.

Matsunami, H., Buck, L.B. 1997. A multigene family encoding a diverse array of putative pheromone receptors in mammals. Cell 90, 775-784.

Min, H., Danilenko, D.M., Scully, S.A., Bolon, B., Ring, B.D., Tarpley, J.E., DeRose, M., Simonet, W.S. 1998. Fgf-10 is required for both limb and lung development and exhibits striking functional similarity to Drosophila branchless. Genes Dev. 12, 3156-3161.

Neumann, H., Schmidt, H., Wilharm, E., Behrens, L., Wekerle, H. 1997. Interferon gamma gene expression in sensory neurons: evidence for autocrine gene regulation. J. Exp. Med. 186, 2023-2031.

Ohuchi, H., Yasue, A., Ono, K., Sasaoka, S., Tomonari, S., Takagi, A., Itakura, M., Moriyama, K., Noji, S., Nohno, T. 2005. Identification of cis-element regulating expression of the mouse Fgf10 gene during inner ear development. Dev. Dyn. 233, 177-187.

Ornitz, D.M., Itoh, N. 2001. Fibroblast growth factors. Genome Biol. 2 (3):REVIEWS3005.

Pauley, S., Wright, T.J., Pirvola, U., Ornitz, D., Beisel, K., Fritzsch, B. 2003. Expression and function of FGF10 in mammalian inner ear development. Dev. Dyn. 227, 203-215.

Powles, N., Babbs, C., Ficker, M., Schimmang, T. and Maconochie, M. 2004. Identification and analysis of genes from the mouse otic vesicle and their association with developmental subprocesses through in situ hybridization. Dev. Biol. 268, 24-38.

Reuss, B., von Bohlen und Halbach, O. 2003. Fibroblast growth factors and their receptors in the central nervous system. Cell Tissue Res. 313, 139-157.

Romand, R., Niederreither, K., Abu-Abed, S., Petkovich, M., Fraulob, V., Hashino, E., Dolle, P. 2004. Complementary expression patterns of retinoid acid-synthesizing and -metabolizing enzymes in pre-natal mouse inner ear structures. Gene Expr. Patterns 4, 123-133.

Ryba, N.J., Tirindelli, R. 1997. A new multigene family of putative pheromone receptors. Neuron 19, 371-379.

Sekine, K., Ohuchi, H., Fujiwara, M., Yamasaki, M., Yoshizawa, T., Sato, T., Yagishita, N., Matsui, D., Koga, Y., Itoh, N., Kato, S. 1999. Fgf10 is essential for limb and lung formation. Nat. Genet. 21, 138-141.

Sharpe, J., Ahlgren, U., Perry, P., Hill, B., Ross, A., Hecksher-Sorensen, J., Baldock, R., Davidson, D. 2002. Optical projection tomography as a tool for 3D microscopy and gene expression studies. Science. 296, 541-545

Shinohara, H., Asano, T. and Kato, K. 1992. Differential localization of g-proteins gi and go in the accessory olfactory bulb of the rat. J. Neurosci. 12, 1275-1279.

Song, Y., Hui, J.N., Fu, K.K., Richman, J.M. 2004. Control of retinoic acid synthesis and FGF expression in the nasal pit is required to pattern the craniofacial skeleton. Dev. Biol. 276, 313-329.

Trauth, K., Mutschler, B., Jenkins, N.A., Gilbert, D.J., Copeland N.G., Klempnauer, K.H. 1994. Mouse A-myb encodes a trans-activator and is expressed in mitotically active cells of the developing central nervous system, adult testis and B lymphocytes. EMBO J. 13, 5994-6005.

Trumpp, A., Depew, M.J., Rubenstein, J.L., Bishop, J.M., Martin, G.R. 1999. Cre-mediated gene inactivation demonstrates that FGF8 is required for cell survival and patterning of the first branchial arch. Genes Dev. 13, 3136-3148.

Verpy, E., Leibovici, M., Petit, C. 1999. Characterization of otoconin-95, the major protein of murine otoconia, provides insights into the formation of these inner ear biominerals. Proc. Natl. Acad. Sci. U S A. 96, 529-534.

Wang, Y., Kowalski, P.E., Thalmann, I., Ornitz, D.M., Mager, D.L., Thalmann, R. 1998. Otoconin-90, the mammalian otoconial matrix protein, contains two domains of homology to secretory phospholipase A2. Proc. Natl. Acad. Sci. USA 95,15345-15350.

Wright, T.J., Mansour, S.L. 2003. Fgf3 and Fgf10 are required for mouse otic placode induction. Development. 130, 3379-3390.

Yang, H., Shi, P., Zhang, Y., Zhang, J. 2005. Composition and evolution of the V2r vomeronasal receptor gene repertoire in mice and rats. Genomics 86, 306-315.

Figure Legends

Figure 1

Selected genes, downregulated in *Fgf3*$^{-/-}$, *Fgf10*$^{-/-}$ and compound *Fgf3*$^{-/-}$/*Fgf10*$^{-/-}$ mouse mutant embryos compared to wild-type embryos at E10. Signal fold changes showing fold-down-regulation between wild-type and mutant samples are indicated.

Figure 2

Downregulation of retinaldehyde-dehydrogenase1, otoconin 90 and vomeronasal receptors (V2Rs) in FGF mutants. Using primers for the indicated genes semi-quantitative RT-PCR was performed from RNA isolated from whole embryos at E10 (A-C) and dorsal root ganglia at E13 (D,E) from embryos with the indicated genotypes. Abbreviations: wt, wild-type; ko3, *Fgf3*$^{-/-}$ mutant; ko10, *Fgf10*$^{-/-}$ mutant; dko, *Fgf3*$^{-/-}$/*Fgf10*$^{-/-}$ mutant.

Figure 3

Expression of vomeronasal recptors (V2Rs) in mouse embryos (A) Embryo at E10 in which the otic vesicle (asterisk) and the area used for the preparation of RNA for the hybridisation of the microarrays are indicated. (B) Dorsal view of an embryo at E10 showing presence of V2R transcripts in the neural tube (nt) and dorsal root ganglia (drg). (C) Horizontal section showing expression of V2Rs in the dorsal part of the neural tube (nt) and dorsal root ganglia (drg) at E10. (D) Section through the developing eye at E10 showing expression of V2R in the retina (r). (E) Coronal section showing expression of V2Rs in the lateral part of the olfactory pit (op) at E10. (F) Coronal OPT section showing expression in the lateral part of the nasal pit (left) and the anlage of the VNO (asterisks) at E11.75. (G) 3D reconstruction of the expression domains of V2R in the nasal pit at E11.75. The medial (m) -lateral (l) axis and the anlage of the VNO is indicated by an asterisk.

Figure 4

Morphology of the vomeronasal organ (VNO) in adult *Fgf3*$^{-/-}$ mouse mutants. Coronal sections through the VNO of an adult wild-type (wt) mouse (A,C) and a *Fgf3*$^{-/-}$ knock-out (ko) mutant (B,D). (A,B) Note the presence of a normally structured VNO in the mutant. (C,D) Coronal sections of the VNO stained with V2R2 antibodies marking vomeronasal receptor neurons in the basal part of the neuroepithelium, characterized by the expression of V2Rs and the G-protein α-subunit $G_{o\alpha}$. Abbreviations: l, lumen; ns non-sensory epithelium; se, sensory epithelium.

Figure

Click here to download high resolution image

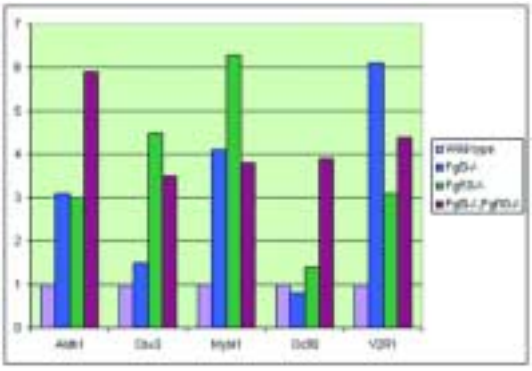

Figure

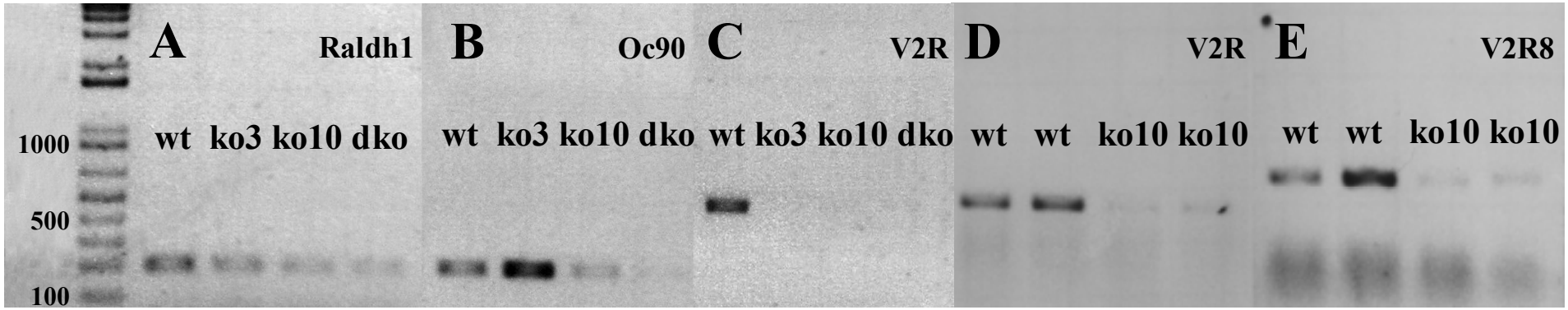
A
Raldh1
wt ko3 ko10 dko
1000
500
100
B
Oc90
wt ko3 ko10 dko
C
V2R
wt ko3 ko10 dko
D
V2R
wt wt ko10 ko10
E
V2R8
wt wt ko10 ko10

Figure

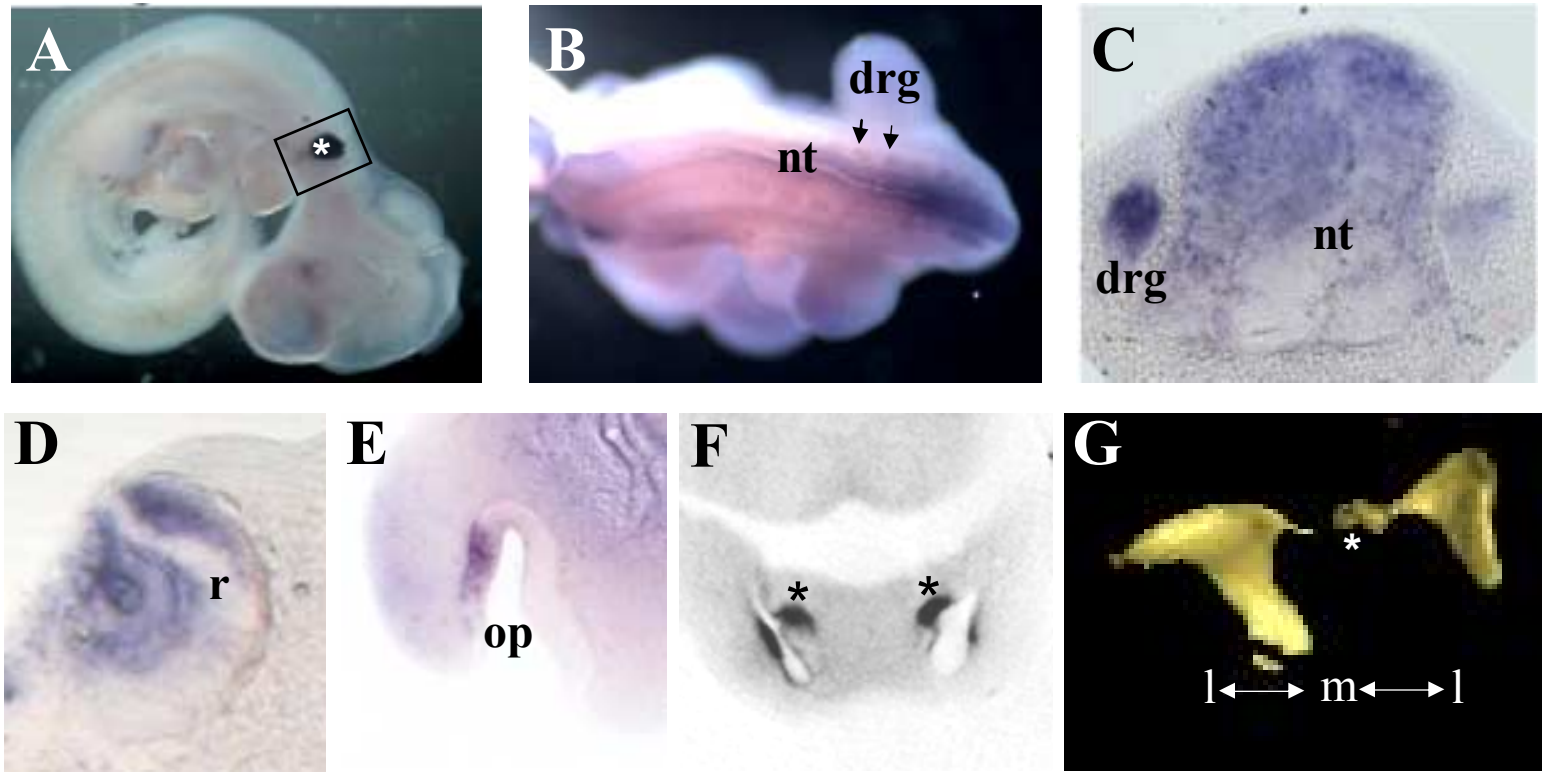

Figure

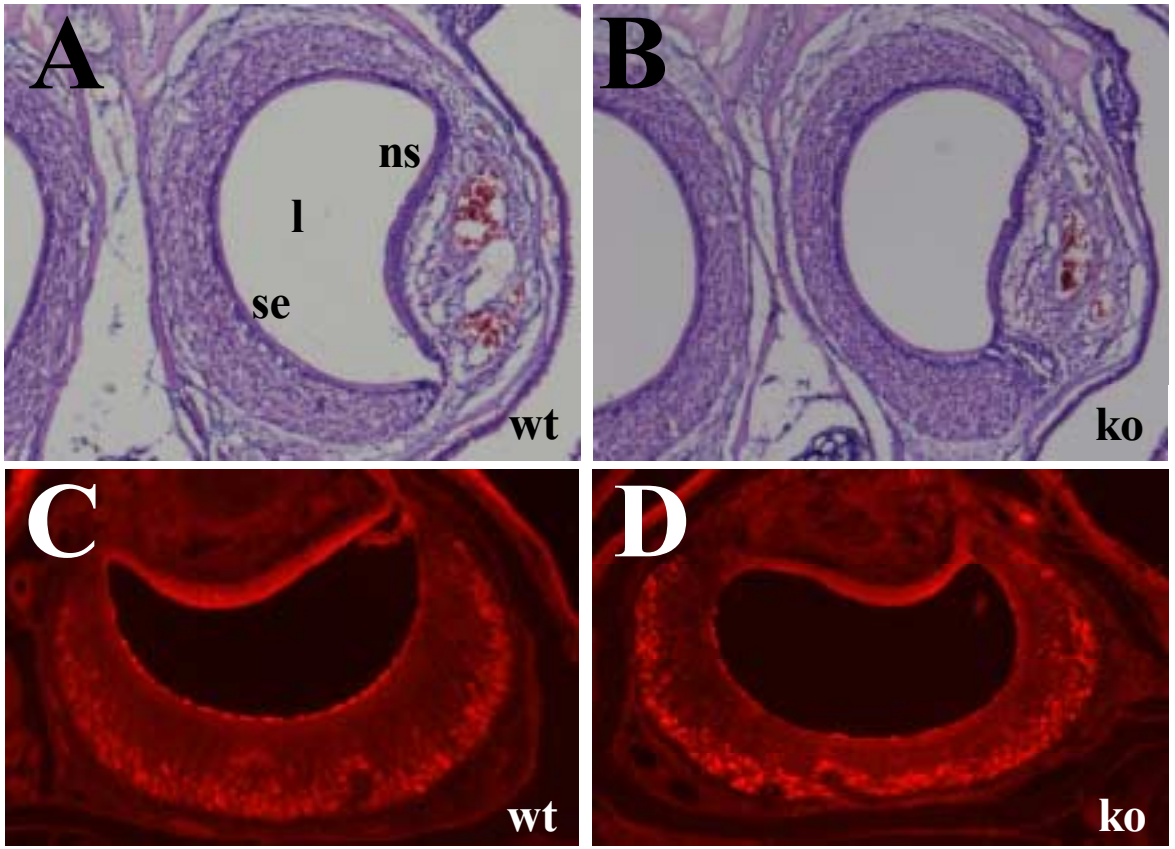

Supplemental

Click here to download Supplemental: wtversusFGF3ko.xls

Supplemental

Click here to download Supplemental: wtversusFGF10ko.xls

Supplemental

Click here to download Supplemental: wtversus FGF3+10ko.xls